

Nicotinamide and pyridoxine stimulate muscle stem cell expansion and enhance regenerative capacity during aging

Sara Ancel, ... , Pascal Stuelsatz, Jerome N. Feige

J Clin Invest. 2024. <https://doi.org/10.1172/JCI163648>.

Research In-Press Preview Muscle biology Stem cells

Skeletal muscle relies on resident muscle stem cells (MuSCs) for growth and repair. Aging and muscle diseases impair MuSC function, leading to stem cell exhaustion and regenerative decline that contribute to the progressive loss of skeletal muscle mass and strength. In the absence of clinically available nutritional solutions specifically targeting MuSCs, we used a human myogenic progenitor (hMP) high-content imaging screen of natural molecules from food to identify nicotinamide (NAM) and pyridoxine (PN) as bioactive nutrients that stimulate MuSCs and have history of safe human use. NAM and PN synergize via CK1-mediated cytoplasmic β -catenin activation and AKT signaling to promote amplification and differentiation of MuSCs. Oral treatment with a combination of NAM/PN accelerates muscle regeneration in vivo by stimulating MuSCs, increases muscle strength during recovery, and overcomes MuSC dysfunction and regenerative failure during aging. Levels of NAM and bioactive PN spontaneously decline during aging in model organisms and independently associate with muscle mass and walking speed in a human cohort of 186 aged people. Collectively, our results establish NAM/PN as a new nutritional intervention that stimulates MuSCs, enhances muscle regeneration, and alleviates age-related muscle decline with a direct opportunity for clinical translation.

Find the latest version:

<https://jci.me/163648/pdf>



1 **Nicotinamide and Pyridoxine Stimulate Muscle Stem Cell Expansion and**
2 **Enhance Regenerative Capacity during Aging**

3
4 **Sara Ancel^{1,2,*}, Joris Michaud^{1,*}, Eugenia Migliavacca¹, Charline Jomard³, Aurélie**
5 **Fessard³, Pauline Garcia^{1,3}, Sonia Karaz¹, Sruthi Raja^{1,2}, Guillaume Jacot¹, Thibaut**
6 **Desgeorges¹, José L Sánchez-García¹, Loic Tauzin⁴, Yann Ratinaud¹, Benjamin Brinon¹,**
7 **Sylviane Métairon⁴, Lucas Pinero¹, Denis Barron¹, Stephanie Blum⁵, Leonidas G.**
8 **Karagounis^{5,6}, Ramin Heshmat⁷, Afshin Ostovar⁷, Farshad Farzadfar⁷, Isabella Scionti³,**
9 **Rémi Mounier³, Julien Gondin³, Pascal Stuelsatz^{1,#}, and Jerome N Feige^{1,2,#}**

10
11 1- Nestlé Institute of Health Sciences, Nestlé Research; Lausanne, Switzerland.

12 2- School of Life Sciences, Ecole Polytechnique Fédérale de Lausanne (EPFL); Lausanne,
13 Switzerland.

14 3- Institut NeuroMyoGène, Unité Physiopathologie et Génétique du Neurone et du Muscle,
15 CNRS, UMR5261, INSERM U1315, Université Claude Bernard Lyon 1, Lyon, France.

16 4- Nestlé Institute of Food Safety & Analytical Sciences, Nestlé Research; Lausanne,
17 Switzerland.

18 5- Translational Research, Nestlé Health Science, Lausanne, Switzerland.

19 6- Mary MacKillop Institute for Health Research (MMIHR), Australian Catholic University,
20 Melbourne, Australia.

21 7- Chronic Diseases Research Center, Endocrinology and Metabolism Population Sciences
22 Institute, Tehran University of Medical Sciences; Tehran, Iran.

23
24 ^{*,#}: these authors contributed equally

25
26 [#] Corresponding authors:

27 Nestlé Research, Building H, EPFL Innovation Park, CH-1015 Lausanne, Switzerland

28 Phone: +41 21 632 6100

29 pascal.stuelsatz@rd.nestle.com; jerome.feige@rd.nestle.com

30 **ABSTRACT**

31 Skeletal muscle relies on resident muscle stem cells (MuSCs) for growth and repair. Aging and
32 muscle diseases impair MuSC function, leading to stem cell exhaustion and regenerative
33 decline that contribute to the progressive loss of skeletal muscle mass and strength. In the
34 absence of clinically available nutritional solutions specifically targeting MuSCs, we used a
35 human myogenic progenitor (hMP) high-content imaging screen of natural molecules from
36 food to identify nicotinamide (NAM) and pyridoxine (PN) as bioactive nutrients that stimulate
37 MuSCs and have history of safe human use. NAM and PN synergize via CK1-mediated
38 cytoplasmic β -catenin activation and AKT signaling to promote amplification and
39 differentiation of MuSCs. Oral treatment with a combination of NAM/PN accelerates muscle
40 regeneration in vivo by stimulating MuSCs, increases muscle strength during recovery, and
41 overcomes MuSC dysfunction and regenerative failure during aging. Levels of NAM and
42 bioactive PN spontaneously decline during aging in model organisms and inter-independently
43 associate with muscle mass and walking speed in a human cohort of 186 aged people.
44 Collectively, our results establish NAM/PN as a new nutritional intervention that stimulates
45 MuSCs, enhances muscle regeneration, and alleviates age-related muscle decline with a direct
46 opportunity for clinical translation.

47

48 **Keywords: stem cells; skeletal muscle; regeneration; nutrition; aging; sarcopenia**

49 INTRODUCTION

50

51 Skeletal muscle is a remarkably plastic tissue that adapts structurally and functionally
52 to lifestyle or external stimuli such as exercise, disuse, or injury. Resident PAX7-expressing
53 muscle stem cells (MuSCs), also known as satellite cells, drive tissue repair during regeneration
54 and directly contribute to muscle growth and long-term muscle maintenance (1, 2). Under
55 homeostatic conditions, MuSCs are maintained in a quiescent state by signals from the local
56 niche that keep them cell-cycle arrested (3). MuSCs are essential to repair myofibers after
57 damage, for which mechanical and inflammatory niche-derived signals stimulate their
58 proliferation and differentiation while also ensuring self-renewal to replenish the pool (1).
59 MuSCs also contribute to myonuclei turnover during homeostasis (4) and can fuse to myofibers
60 to maintain myonuclear domains and support resistance training induced muscle hypertrophy
61 (5, 6). The regulation of MuSC metabolism is critical for their fate as activation and
62 proliferation increase metabolic requirements (7, 8). While changes in macro-nutrient
63 availability have been shown to influence the ability of MuSCs to support regeneration and
64 exercise adaptation (9, 10), the understanding of which individual nutrients from food regulate
65 MuSCs is limited.

66 During aging, skeletal muscle gradually loses its ability to regenerate and muscle mass
67 and strength decline, a condition clinically known as sarcopenia. Sarcopenia is a complex and
68 multifactorial process, involving multiple cellular mechanisms such as impaired
69 neuromuscular junction transmission, myofiber mitochondrial dysfunction, and oxidative
70 stress / inflammation (11), and lifestyle factors linked to nutrition and physical activity (12).
71 The number and regenerative capacity of MuSCs decline during aging and sarcopenia both in
72 animal models and in humans (13, 14). This decline involves a complex interplay of cell-
73 autonomous and niche-dependent mechanisms where MuSC epigenetic and metabolic

74 perturbations cross-talk with altered structural and extracellular signals from myofibers,
75 accessory cells and systemic blood supply (14–21).

76 Several proof-of-concept preclinical studies have shown that age-related MuSC
77 dysfunction can be reversed with blockade of prostaglandin degradation or p38 and JAK-STAT
78 signaling, NAD⁺ precursors, or activators of autophagy, which restore regenerative capacity
79 and improve muscle strength or performance (22–27). While genetic ablation of MuSCs has
80 shown their absolute requirement for muscle regeneration and myofiber recovery (4, 28), life-
81 long MuSC depletion in sedentary mice did not aggravate the age-related loss of muscle mass
82 (29), suggesting that myonuclei accretion via MuSCs may not be a primary driver of
83 sarcopenia. However, functional capacity does not decline linearly during aging in humans,
84 where recovery from acute events is important and mobilizes MuSCs. In particular, micro-
85 injuries caused by physical activity and traumatic events such as surgeries or falls cause a
86 transient decline in muscle mass and function with slow and often sub-maximal recovery
87 during aging (30, 31). This critical window represents an opportunity to accelerate MuSC-
88 mediated muscle repair and prevent long-term aggravation of sarcopenia.

89 While pharmacological strategies to modulate MuSCs are emerging preclinically, their
90 clinical use is often limited by the lack of safety and toxicology studies supporting clinical use
91 and the requirement of regulatory approvals as drugs. Here, we used a high-content imaging
92 screen of a library of natural bioactive molecules and food-derived nutrients on human
93 myogenic progenitors (hMPs) to identify new nutritional molecules targeting MuSCs. Using
94 this approach, we discovered that nicotinamide (NAM) and pyridoxine (PN) are potent
95 nutrients that signal through CK1/β-catenin and AKT to stimulate MuSC proliferation and
96 induce their differentiation. Oral in vivo treatment with NAM/PN enhances MuSC expansion,
97 increases strength recovery and accelerates myofiber repair in young and aged mice as well in
98 primary myogenic cells from aged and geriatric donors. Given that circulating levels of

99 endogenous NAM and bioactive PN are low in older people with reduced muscle mass and
100 function and that both NAM and PN have a history of safe human use, our results provide a
101 new therapeutic solution ready for human clinical use to stimulate muscle regeneration and
102 mitigate age-associated muscle decline.

103 **RESULTS**

104 **A high-content imaging screen identifies NAM and PN as myogenic activators in primary** 105 **human myogenic progenitors**

106 To discover new natural bioactive nutrients that modulate myogenic progenitor
107 function with a relevance for clinical translation, we developed a robust automated high-
108 content imaging screen using primary hMP cells isolated from quadriceps muscles and
109 validated for purity by >99% expression of the myogenic marker CD56 (Fig. S1A). We used
110 hMPs from 2 male and 4 female representative donors that were selected based on purity and
111 myogenic function (donors A,B,C,D,I,J; Table S1). Over 50,000 natural bioactive molecules
112 and plant extracts were screened on a representative hMP donor for amplification of MYOD⁺
113 cells (Fig. 1A, Fig. S1B). In this primary screen, 534 compounds passed the cutoff criteria of
114 increasing by at least 15% the number of differentiating PAX7⁺/MYOD⁺ cells (Fig. 1A, blue
115 datapoints and table S2). Because our focus was on molecules with rapid translational potential,
116 we refined our selection to FDA-approved molecules and identified NAM and PN (Fig. 1A,
117 red datapoints) as the most potent and Generally Recognized As Safe (GRAS) inducers of
118 MYOD in hMPs, with both molecules increasing by ~35% the number of PAX7⁺/MYOD⁺ cells
119 (Fig. 1B).

120 To confirm and deconvolute these results, we analyzed the dose-response relationship
121 of NAM and PN on MYOD and extended the analysis to PAX7. NAM and PN increased the
122 number of MYOD⁺ hMPs starting at 110 μ M (Fig. 1C,D), and this effect was conserved across
123 the 3 other young hMP donors (Fig. S1C). Only NAM concomitantly increased the number of
124 PAX7⁺ and Ki67⁺ cells (Fig. 1E and Fig. S1D-F). The effects of NAM on the number of
125 MYOD⁺ cells resulted primarily from early effects on proliferation as the relative number of
126 MYOD⁺ cells normalized to total or proliferating cell number was only modestly affected by
127 NAM (Fig. S1G,H). In contrast, PN increased the percentage of MYOD⁺ cells normalized to

128 total or proliferating cells (Fig. S1I,J), indicating that PN induces differentiation independently
129 of proliferation. To understand the molecular basis of each molecule, we analyzed the
130 transcriptome of vehicle, NAM-, PN- and NAM/PN-treated hMPs (Fig. 1F-I, Fig. S1K-M and
131 table S3-4). Gene set enrichment analysis (GSEA) revealed upregulation of pathways involved
132 in cell cycle progression and cell division following treatment with NAM (Fig. 1F), as expected
133 from the increase in the number of proliferating progenitors (Fig. 1E and Fig. S1E). PN-treated
134 hMPs had a strong signature of protein synthesis (Fig. 1G), consistent with myogenic
135 differentiation requiring increased protein translation (32). While both NAM and PN increased
136 the number of MYOD⁺ hMPs, transcriptomic and phenotypic analyses suggested that both
137 molecules modulate different, complementary myogenic functions in vitro. When combining
138 NAM and PN treatments, the individual transcriptional signature of each molecule was
139 conserved (Fig. 1F-H, S1K-M). Notably, 630 genes were differentially upregulated by the
140 NAM/PN combination over single treatments (Fig. 1I; table S4), highlighting that NAM and
141 PN synergize to regulate hMP gene expression. At the phenotypic level, compared to hMPs
142 treated with NAM or PN alone, the NAM/PN combination synergistically increased the number
143 of MYOD⁺ cells and improved both the EC50 and the maximal efficacy over the effects of
144 single treatments (Fig. 1J). The NAM/PN combination also maintained the ability to stimulate
145 PAX7⁺ hMP proliferation (Fig. 1K) and enhanced terminal differentiation and myotube
146 maturation (Fig. 1L-O and Fig. S1N-P). The effects of NAM/PN on differentiation resulted
147 from early-stage hMP amplification and were not observed when NAM/PN was supplemented
148 after myotube formation was induced (Fig. S1Q-U). An important feature of MuSC fate is the
149 capacity to concomitantly engage in myogenic differentiation while self-renewing a pool of
150 cells that maintains stemness. This process can be modeled in vitro by assessing the capacity
151 of myoblasts to form PAX7⁺ reserve cells via niche signals derived from myotubes during
152 differentiation (33). To test if NAM/PN regulates self-renewal independent of its effect on

153 MuSC proliferation and differentiation, we analyzed reserve cells in hMPs treated with
154 NAM/PN after the induction of myotube differentiation. The effects of NAM/PN on
155 proliferation and differentiation (Fig. 1C-E) did not come at the expense of self-renewal as
156 NAM/PN actually increased the number of PAX7⁺ reserve cells after differentiation (Fig. 1P).
157 We also tested if NAM/PN cross-talks with cell proliferation of other human cells with high
158 proliferation rates. The effects on hMP amplification were specific to myogenic progenitors
159 and not recapitulated in non-myogenic cells as NAM/PN did not stimulate proliferation of skin
160 fibroblasts, unlike the positive control FGF (Fig. S1V,W). Altogether, our in vitro results
161 demonstrate that NAM and PN can be combined to stimulate myogenesis by modulating both
162 myogenic progenitor proliferation and differentiation specifically.

163

164 ***In vivo* NAM/PN treatment stimulates MuSCs, accelerates regeneration and increases** 165 **muscle strength after muscle injury**

166 To evaluate if NAM/PN can support MuSCs in a complex physiological system and
167 across species, lineage-negative (CD31⁻/CD45⁻/CD11B⁻/SCA1⁻) and CD34⁺/ITGA7⁺ MuSCs
168 were isolated from mouse hindlimb muscles by FACS and treated ex vivo with NAM/PN.
169 NAM/PN increased the total number of PAX7⁺, as well as the PAX7⁺/EdU⁺ proliferating
170 MuSCs (Fig. 2A-C) and stimulated their progression towards MYOD⁺ progenitors (Fig. 2A,D).
171 To substantiate these results in vivo, we analyzed MuSC function in a preclinical model of
172 muscle regeneration after an acute muscle injury induced with cardiotoxin (CTX) (Fig. 2E).
173 Following oral administration, NAM and PN were well absorbed and bioavailable in skeletal
174 muscle as both their circulating (Fig. S2A) and intramuscular levels (Fig. 2F,G) were strongly
175 increased compared to the vehicle-treated group. The NAM/PN treatment was also well
176 tolerated with no sign of toxicity (Fig. S2B-D).

177 NAM/PN supplementation significantly increased by 38% the number of PAX7⁺
178 MuSCs and the number of proliferative PAX7⁺ cells measured via Ki67 at 5 days post injury
179 (dpi) (Fig. 2H-J). Consistent with the effects of NAM and PN on early markers of
180 differentiation in cell culture (Fig. 1C,D and 2A,D), NAM/PN also increased the number of
181 differentiating MYOGENIN⁺ progenitors in vivo (Fig. 2H,K). To ensure that NAM/PN did not
182 perturb MuSC self-renewal in vivo, we quantified return to quiescence once the majority of
183 differentiation and self-renewal decisions have occurred. NAM/PN did not affect return to
184 quiescence as the number of non-cycling sublaminal PAX7⁺ MuSCs in regenerating areas did
185 not differ between vehicle- and NAM/PN-treated muscle at 12 dpi (Fig. 2L). The acceleration
186 of myogenic repair translated into increased regenerating myofiber size at 12 dpi with a 6.2%
187 shift towards larger more mature fibers (Fig. 2M-P and S2E). Altogether, these results indicate
188 that NAM/PN enhances muscle regeneration in vivo in young healthy conditions by
189 accelerating MuSC dynamics and fiber repair without compromising self-renewal.

190 To investigate the functional relevance of NAM/PN during muscle recovery, we
191 measured muscle strength in a physiological mouse model of skeletal muscle regeneration
192 induced by eccentric exercise using a standardized electrically evoked lengthening contraction
193 protocol (Fig. 2Q; (34)). Consistent with the results in the severe model of CTX-induced
194 muscle regeneration (Fig. 2H-K), NAM/PN also increased the proliferation of PAX7⁺ MuSCs
195 and their myogenic differentiation to MYOGENIN⁺ in this milder model of contraction-
196 induced regeneration (Fig. 2R-U). Muscle strength was recorded longitudinally using a non-
197 invasive set-up where evoked contraction recorded on a foot pedal was measured one day after
198 injury, during the dynamic myofiber remodeling phase at 7 dpi and during the fiber maturation
199 process at 14 dpi (Fig. 2Q). Following eccentric contraction-induced injury, muscle strength
200 dropped by 50% and gradually recovered across the 14-day time course (Fig. 2V). Muscle
201 strength was 27% higher in NAM/PN compared to vehicle-treated animals at 7 dpi, and this

202 difference was maintained at 14 dpi, enabling a more rapid return to pre-injury strength levels
203 (Fig. 2V). These results across independent models of regeneration demonstrate that NAM/PN
204 supports all phases of muscle repair by boosting the initial amplification of MuSCs and
205 inducing their progression toward differentiation, resulting in better muscle strength
206 throughout the entire recovery process.

207

208 **NAM and PN signal through selective CK1-mediated β -catenin activation independent of** 209 **NAD⁺ metabolism, and AKT signaling, respectively**

210 Given the role of NAM as an NAD⁺ precursor and the importance of NAD metabolism
211 in skeletal muscle homeostasis and regeneration (24, 35), we examined the potential of
212 increasing endogenous NAD⁺ levels to stimulate MuSCs. Treatment of hMPs with the NAD⁺
213 precursors NAM, nicotinamide riboside (NR), and nicotinamide mononucleotide (NMN) (Fig.
214 3A), resulted in comparable increases of NAD⁺ levels (Fig. 3B). However, only NAM
215 increased the number of PAX7⁺ and Ki67⁺ hMPs (Fig. 3C,D). To confirm these in vitro
216 findings, we compared the effects of NAM and NR on muscle regeneration in vivo and
217 evaluated whether boosting NAD⁺ levels in healthy muscle was sufficient to enhance MuSC
218 function. Supplementation with NR and NAM increased the NAD⁺ content in muscle to a
219 similar extent (Fig. S3A), but only NAM increased the number of PAX7⁺, Ki67⁺, and
220 MYOGENIN⁺ progenitors (Fig. 2H-K and Fig. S3B-E), suggesting that the amplification of
221 myogenic progenitors is NAM-specific. Since NR has been reported to convert to NAM via
222 the enzyme Pnp in mammals (36, 37), we assessed NAM levels following NR supplementation
223 in mice (Fig. S3F,G). As expected, circulating levels of NAM increased following NR
224 administration but the circulating levels of NAM resulting from NR conversion were 50 times
225 lower compared to the levels reached after NAM/PN supplementation (Fig. S3F). Unlike oral
226 NAM/PN, NAM conversion following oral NR was not sufficient to increase NAM

227 bioavailability in skeletal muscle (Fig. S3G). To further validate that NAM promotes myogenic
228 cell proliferation independently of NAD⁺, we blocked the conversion of NAM to NAD⁺
229 through inhibition of NAMPT with FK-866. As expected, FK-866 inhibited the conversion of
230 NAM to NAD⁺ (Fig. 3E), but did not abolish the expansion of PAX7⁺ and Ki67⁺ hMPs by
231 NAM (Fig. 3F,G). In addition to its role as an NAD⁺ precursor, NAM has previously been
232 shown to signal via NAD-independent mechanisms at high concentrations (38). We therefore
233 examined the impact of different doses of NAM on hMP proliferation and NAD⁺ biosynthesis
234 (Fig. 3H-K). While both concentrations of NAM triggered a comparable increase in NAD⁺
235 levels (Fig. 3I), only high concentrations of NAM enhanced hMP proliferation (Fig. 3H,J,K).
236 Collectively, our in vitro and in vivo data demonstrate that increasing NAD⁺ alone is not
237 sufficient to improve the function of young healthy MuSCs and suggest that NAM can activate
238 MuSCs independently of NAD⁺.

239 NAM inhibits casein kinase 1 alpha (CK1 α) activity (Fig. 4A) (33) at doses stimulating
240 myogenic cell proliferation (Fig. 4A and 1D). Hyperactivation of CK1 drastically decreased
241 the number of proliferating hMPs and was dominant over NAM, while both NAM and the
242 pharmacological CK1 inhibitor increased hMP proliferation (Fig. 4B-D). These results
243 demonstrate that CK1 is a regulator of MuSC proliferation and that NAM signals in hMPs via
244 CK1 inhibition.

245 In non-myogenic cells, CK1 α directly phosphorylates cytoplasmic β -catenin to inhibit
246 its activity by inducing proteosomal-mediated degradation (39). CK1 can also inhibit β -catenin
247 in hMPs, as pharmacological CK1 hyperactivation increased phosphorylated inactive β -catenin
248 (Fig. S4A,B). Similar to NAM, pharmacological CK1 inhibition increased the number of
249 proliferating Ki67⁺ and PAX7⁺ hMPs (Fig. S4C-D). As expected, the canonical positive control
250 WNT3A strongly increased active non-phosphorylated β -catenin. In line with its inhibition of
251 CK1 (Fig 4A), NAM also increased active β -catenin 1.6 fold in hMPs to a smaller extent than

252 WNT3A (Fig 4E,F). To directly measure β -catenin transcriptional activity in MuSCs, we
253 performed a luciferase reporter assay on freshly isolated MuSCs co-transfected with the
254 TopFlash luciferase β -catenin reporter as previously described (40). 72h of NAM treatment
255 increased β -catenin transcriptional activity by 66% (Fig. 4G), demonstrating that the NAM-
256 driven accumulation of β -catenin stimulates β -catenin dependent target gene activation.

257 Following translocation to the nucleus, active β -catenin interacts with two
258 acetyltransferases, cAMP response element binding protein (CREB)-binding protein (CBP)
259 and E1A-binding protein, 300 kDa (p300) to drive the expression of its target genes (41). To
260 better understand how NAM modulates β -catenin signaling, hMPs were treated with ICG-001
261 and IQ-1, two β -catenin antagonists that prevent the transcription of sets of β -catenin-
262 dependent genes by disrupting the interaction between β -catenin and its co-activators CBP or
263 p300, respectively (42, 43). Inhibition of the β -catenin/p300 interaction with IQ-1 did not
264 impact basal or NAM-induced proliferation of hMPs (Fig. 4H-J). In contrast, inhibition of the
265 β -catenin/CBP interaction with ICG-001 strongly decreased hMP proliferation and completely
266 blocked the ability of NAM to stimulate hMP proliferation (Fig. 4H-J) without affecting cell
267 viability or the ability to respond to the TGF β inhibitor used as positive control (Fig. S4C). As
268 an additional control, we verified that neither ICG-001 nor IQ-1 affected the capacity of PN to
269 upregulate MYOD in hMPs (Fig. S4D,E). These results suggest that NAM signals by activating
270 a set of β -catenin target genes that is specifically regulated by the association with its co-
271 activator CBP and demonstrate that NAM induces myogenic cell proliferation independent of
272 NAD⁺ via a partial activation of β -catenin signaling via cytoplasmic CK1-mediated inhibition.

273 The AKT serine/threonine kinase controls myogenic differentiation and is a central
274 regulator of anabolic processes and muscle protein synthesis (44), which were regulated in
275 hMPs in response to PN (Fig. 1G). Consistent with these transcriptomic profiles, PN treatment
276 in hMPs increased the expression of the active phosphorylated form of AKT (Fig. 4K,L). AKT

277 inhibition using the allosteric inhibitor MK-2206 decreased the number of MYOD⁺ cells (Fig.
278 4M,N). Importantly, the effects of PN were fully dependent on AKT as AKT and PI3K
279 inhibitors completely abolished the PN-induced upregulation of MYOD⁺ cells (Fig. 4M,N and
280 Fig. S4F), while maintaining sensitivity to the TGF- β inhibitor as positive control for myogenic
281 induction (Fig. S4F). Moreover, treatment with an AKT activator mimicked the effect of PN
282 on MYOD in hMPs (Fig. S4G-I). As a control, we also verified that AKT inhibition by MK-
283 2206 did not compromise the effect of NAM on hMP proliferation (Fig. S4J-L).

284 Finally, to confirm that the molecular mechanisms of NAM and PN were conserved in
285 vivo, we isolated activated MuSCs from regenerating muscles 5 dpi with and without oral
286 NAM/PN supplementation and analyzed them by quantitative capillary Western Blot (Fig. 4O-
287 R). Consistent with what we previously observed in hMPs, active β -catenin also accumulated
288 in activated MuSCs from NAM/PN-treated mice (Fig. 4O,P). Moreover, the acetylation of
289 lysine 49 on β -catenin, which is a of readout CBP-mediated activation of β -catenin (45), was
290 also higher in NAM/PN-treated MuSCs (Fig. 4O,Q). Lastly, AKT signaling was also
291 upregulated in freshly-isolated MuSCs following NAM/PN supplementation in vivo (Fig. 4O,
292 R). Altogether, these molecular studies demonstrate that NAM and PN synergize to regulate
293 MuSC proliferation and differentiation in hMPs and MuSCs in vivo through partial CK1-
294 dependent β -catenin activation by NAM independently of NAD⁺, and AKT activation by PN.

295

296 **NAM/PN supplementation reverses MuSC dysfunction and regenerative decline during** 297 **aging**

298 Since aging causes functional decline of MuSCs and defective regeneration, we next
299 evaluated whether endogenous NAM/PN levels are altered during aging and if supplementation
300 of NAM/PN can rescue MuSC function and ameliorate muscle repair in aged mice. NAM and
301 PN levels declined spontaneously during aging with muscle concentrations reduced in aged

302 compared to young mice by 18% and 37%, respectively (Fig. 5A). A comparable 25-35% age-
303 related decrease of NAM and pyridoxal-5'-phosphate (PLP), the bioactive form of PN, was
304 also observed in plasma (Fig. 5B), highlighting that aging causes a global systemic decline of
305 NAM and PN metabolism. Oral NAM/PN supplementation could overcome this age-related
306 deficit (Fig. S5A,B), demonstrating that the intestinal absorption of NAM and PN is not
307 impaired during aging.

308 After CTX-induced muscle injury in aged mice (Fig. 5C), NAM/PN treatment was
309 dominant over age-related impairments of MuSCs. The number of PAX7⁺ MuSCs decreased
310 by 43% in aged muscle at 5 dpi and was fully rescued by NAM/PN treatment (Fig. 5D,E).
311 PAX7⁺ cell amplification was driven by a regulation of MuSC proliferation as the number of
312 PAX7⁺/Ki67⁺ cells decreased significantly during aging and was rescued by NAM/PN (Fig.
313 5D,F). NAM/PN also increased the number of MYOGENIN⁺ cells at 5 dpi in aged muscle,
314 thereby mitigating the age-related defects in myogenic progenitor differentiation (Fig. 5D,G).
315 We next evaluated the transcriptional changes induced by NAM/PN in MuSCs freshly isolated
316 from aged mice or in aged regenerating muscle from NAM/PN-treated mice. When compared
317 to young MuSCs, pathways involved in MuSC proliferation and differentiation were
318 downregulated in aged MuSCs, and re-activated in aged MuSCs treated with NAM/PN (Fig.
319 5H). Aging disrupted molecular signatures involved in inflammation, metabolism, and muscle
320 repair in regenerative muscle (46), and these alterations were reversed by NAM/PN treatment
321 (Fig. 5I). Importantly, NAM/PN had minimal impact on the transcriptional landscape of
322 uninjured muscle and did not significantly reverse aging signatures of uninjured muscle (Fig.
323 S5C), suggesting that NAM/PN primarily cross-talks with repair mechanisms in regenerating
324 muscle. Gene expression signatures also suggested that NAM/PN treatment could reduce the
325 expression of pro-fibrotic genes in aged regenerating muscle (Fig. S5D). However, acute
326 NAM/PN treatment during regeneration did not affect fibrosis measured by aniline blue

327 staining in neither regenerating nor uninjured muscles (Fig. 5J,K & S5E-F), suggesting that
328 NAM/PN exerts its beneficial effects primarily by enhancing MuSC function and may fine tune
329 extra-cellular matrix remodeling without acute functional consequences on fibrosis. The
330 enhanced MuSC function in aged muscle with NAM/PN translated into enlarged regenerating
331 myofibers with centralized nuclei at 12 dpi (Fig. 5L-O), with a 25% increase in the number of
332 larger more mature fibers in NAM/PN-treated mice that translated in an overall increase in the
333 myofiber area distribution of 7.6% (Fig. 5O and S5G). No fiber size differences were observed
334 between vehicle- and NAM/PN-treated mice in uninjured contralateral muscles (Fig. S5H-J).
335 Our molecular and histological results thus demonstrate that NAM/PN reverses the aging
336 phenotype of MuSCs and mitigates muscle aging specifically in conditions where MuSCs are
337 active.

338

339 **NAM and PN are reduced in older people with impaired physical function and reverse** 340 **human age-related myogenic decline**

341 To investigate the relevance of NAM and PN for human muscle physiology during
342 aging, concentrations of NAM and PLP, the active form of PN, were measured in the serum of
343 186 randomly selected older men aged 60 years and above from the Bushehr Elderly Health
344 (BEH) program ((47); table 1). In this cohort with a 46% prevalence of sarcopenia (table 1),
345 circulating concentrations of NAM and PLP were low in individuals with low muscle mass
346 assessed via the appendicular lean mass index (ALMi) measured by DXA, and significantly
347 associated with ALMi across all individuals (Fig. 6A and table S5). Similar associations were
348 observed with total ALM (table S5), while normalization to BMI reduced these associations
349 likely because it introduced more variability in the assessment of lean mass. Circulating levels
350 of other hydrosoluble vitamins with similar metabolism and physicochemical properties such
351 as Thiamin (vitamin B1) and Riboflavin (vitamin B2) were not associated with muscle mass

352 measured via the ALMi (Fig. S6A,B), demonstrating that the clinical association of NAM and
353 PN with muscle mass is not an indirect consequence of lower capacity to store micronutrients.
354 Gait speed, a validated clinical variable to assess muscle function which predicts quality of life
355 and mortality (48), was also positively associated with circulating levels of PLP and to a lesser
356 extent of NAM (Fig. 6B). We then used statistical models to evaluate potential dietary causes
357 of the associations as well as functional inter-dependencies of NAM, PLP and age. ALMi and
358 gait speed did not associate with dietary intake of vitamin B3 and B6 measured via food
359 frequency questionnaires, but remained significantly correlated with serum levels of NAM and
360 PLP when the statistical models were corrected for dietary intake (Table S6). A biostatistical
361 model using multiple linear regression adjusted for age demonstrated that NAM and PLP levels
362 directly associate with ALMi and gait speed in all decades analyzed from 60 to 80 years,
363 regardless of the extent of functional decline with age (Fig. 6C,D). Importantly, the
364 contributions of NAM and PLP were interdependent and additive at all ages tested,
365 demonstrating that there is a functional interaction between the levels of NAM and PLP in
366 humans to influence physical capacity.

367 Reduced myogenic capacity during aging is a hallmark of human sarcopenia (12, 47),
368 and was recapitulated in hMPs from 4 young and 4 aged individuals (Fig. 6E-H, Fig. S6C-D
369 and table S1). Treatment with NAM/PN could counteract human age-related myogenic decline
370 by increasing the proliferation of aged PAX7⁺ hMPs (Fig. 6E-G and Fig. S6F-G), their
371 activation of MYOD (Fig. 6H) and their terminal differentiation to myotubes (Fig. S6K-N).
372 The effect size of NAM/PN on myogenic readouts was equivalent in all donors and ages tested
373 (Fig. S6H-J). Altogether, our results on clinical cohorts and primary human cells demonstrate
374 that NAM and PN are clinically relevant nutrients which decline in human sarcopenia and
375 reverse the myogenic defects of aged human myogenic cells.

376 **DISCUSSION**

377 We used a high-content imaging screen on human myogenic progenitors and identified
378 NAM and PN as nutrients that enhance MuSC proliferation and myogenic regeneration. NAM
379 and PN have been recognized as safe by the FDA and EFSA (49, 50) and are approved for
380 broad use in foods or dietary supplements. Targeting MuSC with safe nutritional solutions is
381 particularly relevant to accelerate physiological muscle recovery during MuSC-mediated repair
382 of myofiber micro-damage following exercise, sports-induced muscle tears and injuries or
383 following surgical procedures that mechanically rupture myofibers (5, 51). MuSCs are also
384 impaired in genetic and chronic muscles diseases such as aging, dystrophies, cancer cachexia
385 or diabetes (52–54). The activation of MuSCs by NAM/PN, which enhances regeneration and
386 accelerates the recovery of muscle strength, is therefore a potent therapeutic solution with
387 potential broad applications in the management of healthy healing processes, exercise
388 adaptations, as well as prevention and nutritional management of muscle wasting disorders.

389 The efficacy of NAM/PN involves complementary molecular mechanisms that
390 synergistically enhance proliferation and myogenic capacity of MuSCs. PN stimulates MuSC
391 differentiation by accelerating MyoD activation via AKT signaling and protein synthesis.
392 While stimulation of protein synthesis is important for MuSC differentiation (9), conversion of
393 PN to its bioactive form PLP also catalyzes several rate-limiting reactions for energy
394 metabolism (55), which may also contribute to myogenic fate directly or synergize with Akt
395 signaling as also reported in other tissues and species (56–58). Further analyses will be
396 important to understand if PN activates PI3K/AKT signaling via a specific molecular target or
397 enhances AKT signaling and myogenic differentiation secondary to metabolic adaptations via
398 PLP-sensitive enzymes. NAM is a precursor for the critical cellular cofactor NAD⁺ and is
399 incorporated into NAD⁺ from dietary sources or intracellular metabolism via the salvage
400 pathway (59). Our *in vivo* studies of healthy young mice showed that, unlike NR which

401 contributes to NAD⁺ homeostasis in conditions of NAD⁺ deficiency during aging or disease
402 (24), stimulation of MuSC proliferation by NAM did not require conversion to NAD⁺. While
403 NR has been shown to convert to NAM via hepatic metabolism (60) and this conversion could
404 be detected in vivo during regeneration, the levels of NAM generated from NR were
405 insufficient to stimulate healthy MuSC proliferation. In contrast, NAM stimulates MuSC
406 proliferation via a selective activation of cytoplasmic β -catenin signaling via de-repression of
407 CK1 α -mediated phosphorylation, which facilitates β -catenin acetylation and nuclear
408 translocation. Similar to NAM, pharmacological modulation of CK1 α modulated hMP
409 proliferation, and treatment with a CK1 α activator blocked the effects of NAM. Inhibition of
410 β -catenin interaction with its co-activator CBP, but not p300, abrogated the effects of NAM on
411 PAX7⁺ cells, highlighting that MuSCs are also sensitive to the NAM-dependent selective
412 recruitment of coactivators to β -catenin observed in other lineages (61). Previous studies have
413 suggested that the cross-talk of β -catenin signaling with myogenesis is complex. While
414 activation of canonical Wnt signaling during skeletal muscle repair is well established (62, 63),
415 the role of β -catenin in myogenesis is debated (62–66) and depends on diverse spatio-temporal
416 signals across cellular compartments and cell types. Genetic deletion of β -catenin in MuSCs
417 originally suggested that β -catenin is dispensable for regeneration (64). However, several
418 subsequent studies using mice with constitutively active or knockout β -catenin have shown that
419 β -catenin signaling can modulate MuSC function and impact regeneration (40, 62, 63, 65, 66).
420 The different phenotypes reported upon β -catenin modulation with various tools highlight that
421 this pathway integrates multiple inputs with different sensitivity and that permanent genetic
422 deletion/over-expression of β -catenin leads to different molecular and phenotypic outcomes
423 compared to pharmacological inhibition using Wnt ligands or secreted Frizzled-related
424 proteins. While our findings suggest that a mild and transient activation of cytoplasmic β -
425 catenin via CK1 α inhibition and CBP recruitment is beneficial and supports MuSC

426 proliferation, NAM treatment in genetic models where CK1 or β -catenin is specifically ablated
427 in MuSCs or where specific β -catenin/CBP interaction sites are mutated will be important to
428 confirm the molecular mechanisms through which NAM cross-talks with MuSC proliferation
429 and improves regeneration.

430 In our study, levels of NAM and PN associated with muscle decline during aging and
431 NAM/PN treatment at therapeutic doses could overcome the detrimental effects of aging on
432 MuSC exhaustion and regenerative decline (15). In addition to stimulating healthy MuSCs,
433 NAM/PN treatment reversed the defective proliferation and MYOD activation of aged MuSCs,
434 and enhanced regeneration. NAM/PN also rescued the impaired proliferation and
435 differentiation of hMPs from aged and geriatric humans, demonstrating that the myogenic-
436 activating mechanisms of NAM/PN were dominant over the pathways that decline during aging
437 in rodent and human muscle. Several lines of evidence support that the benefits of NAM/PN
438 supplementation on age-related muscle decline cross-talk with myogenic repair mechanisms.
439 Improved myofiber size and reversal of transcriptomic signatures of aging were specific to
440 regenerating muscle, but were not or minimally affected in uninjured muscle. In addition,
441 NAM/PN enhanced myogenic differentiation when myogenic progenitors were treated but did
442 not affect terminal myotube maturation in vitro. While these results are consistent with a
443 positive effect of NAM/PN on muscle regeneration via myogenic stimulation of MuSCs and
444 their progeny, NAM/PN may also affect non-myogenic cells of the niche that support muscle
445 regeneration (16) and enhance repair mechanisms directly in myofibers (67). Further studies
446 using MuSC-depleted mice will therefore be important to test whether NAM/PN may also
447 support muscle health by stimulating complementary MuSC-independent mechanisms.

448 In our epidemiology study, low circulating levels of NAM and the bioactive form of
449 PN associated with reduced muscle mass and gait speed in older people. Since muscle mass
450 and gait speed are clinical variables used to define sarcopenia and established predictors of

451 physical fitness, quality of life, and survival (12), our results suggest that endogenous
452 inadequacy of these metabolites could contribute to loss of functional capacity during aging.
453 Dietary intake does not seem to be the primary cause linking endogenous NAM/PN levels to
454 muscle health and the association of both nutrients in serum with muscle mass and function
455 was inter-dependent, suggesting that altered endogenous metabolism of these nutrients during
456 aging could explain their association with muscle phenotypes. Impaired regeneration and poor
457 recovery from acute traumatic events such as injuries, surgeries or falls is an important
458 contributing mechanism to the progression of sarcopenia (12). Given the indispensable role of
459 MuSCs in regeneration and recovery from myofiber injury, it is possible that low levels of
460 NAM and PN contribute to sarcopenia via a regenerative mechanism through MuSCs.
461 However, we could not collect muscle biopsies to quantify MuSCs in this clinical study and
462 could therefore not relate clinical outcomes to MuSC activation. Since NAM and PN regulate
463 general metabolic pathways across different cell types, it is possible that NAM and PN may
464 associate with muscle mass and function via an effect in myofibers or other cell types.
465 Collectively, our results support a translational application of NAM/PN in older people with
466 physical decline, especially during the phases of acute recovery. However, sarcopenia has
467 multi-factorial origins, and it will be important to combine NAM/PN with physical activity and
468 other nutrients such as protein, vitamin D and Omega 3 fatty acids which are part of standard
469 of care to manage different physiological mechanisms that contribute to sarcopenia.

470 In summary, NAM/PN supplementation is an effective therapeutic strategy to stimulate
471 MuSCs . Our work in preclinical models, primary human cells and in an observational clinical
472 cohort further establishes NAM/PN as a new translational solution to accelerate skeletal muscle
473 repair and mitigate age-associated regenerative decline by targeting MuSC activation via
474 regenerative nutrition.

475 **MATERIALS AND METHODS**

476 The detailed experimental procedures and reagents utilized in this study are described in the
477 Supplemental Methods section.

478

479 **Sex as a biological variable**

480 For human cells, hMPs from both male and female donors were used (Table S1). All mouse
481 experiments were performed using male mice to maintain consistency throughout the study as
482 aged female mice were not commercially available from the supplier. The nutritional
483 observational study from the Bushehr cohort was analyzed in men to maximize statistical
484 power given gender differences in micro-nutrients during aging (68).

485

486 **Primary human myogenic progenitors (hMPs)**

487 Primary human myogenic progenitors (hMPs, Lonza, #CC-2580 or Cook Myosite, SK-111,
488 table S1) were selected for myogenic purity (>90% desmin-positive cells, CD56 positive) and
489 absence of fibroblast contamination (<5% alpha smooth muscle actin-positive cells). We also
490 controlled all hMPs for their capacity to differentiate into myotubes with a fusion Factor >50%
491 assessed by myosin heavy chain or troponin T. For each experiment, a frozen stock of hMPs
492 cells banked with less than 4 passages was thawed and expanded in Skeletal Muscle Cell
493 Growth Medium (AmsBio, #SKM-M) in a humidified incubator at 37°C in 5% CO₂. hMPs
494 were cultured for a maximum of 3 passages prior to cellular assays and were passaged upon
495 reaching 50-60% confluence, approximately every 3 days.

496

497 **High throughput imaging phenotypic assay**

498 An automated high throughput imaging phenotypic assay was developed to assess hMP
499 proliferation in 384-well plates. All liquid dispensing, compound treatment, and imaging steps

500 were conducted on automated platforms optimized for this screen. A primary screen of 50'000
501 natural bioactive molecules and plant extracts from in-house libraries was performed on Donor
502 A using the percentage of PAX7/MYOD⁺ cells as primary readout. Assay conditions were
503 optimized using the TGFβ inhibitor LY364947 (Sigma, #L6293; (69)) as a positive control to
504 reach an average Z' factor above 0.5. Each 384-well plate contained 320 treatment conditions
505 each tested at 10μM in 1% DMSO, 32 vehicle controls with 1% DMSO only and 32 positive
506 controls treated with 25 μM LY364947 in 1% DMSO. The percentage of PAX7/MYOD⁺ cells
507 was normalized using the Min-Max scaling method with “0” being attributed to the negative
508 control and “1” to the positive controls and results were displayed and analyzed using the
509 Vortex software. All compounds classified by the FDA as Generally Recognized As Safe or
510 “GRAS” were tested at 1 mM for the primary screening and then separately tested for
511 confirmation in duplicates on hMPs from two donors. 800 Cells were plated on 384-well plates
512 pre-coated with 10μg/ml human fibronectin (Corning, #356008) fibronectin and grown in
513 Skeletal Muscle Cell Growth Medium (AmsBio, #SKM-M) for 72 h under humidified
514 conditions at 37°C in 5 % CO₂ before immunocytochemistry and image acquisition, performed
515 as described in the Supplementary Information.

516

517 **Secondary hMP proliferation and differentiation assays**

518 Primary cells were cultured as previously described (70) and experimental procedures and
519 reagents used in this section are detailed in the Supplementary Information. Secondary
520 proliferation and differentiation assays were performed using hMPs from a total of five
521 independent donors (Table S1). Unless otherwise stated, the concentration used for the
522 different treatments were: 1% DMSO as vehicle condition, 1 mM NAM (Nicotinamide,
523 Enamine #EN300-15612), 1mM PN (Pyridoxine, Enamine #EN300-39851), 1 mM NR
524 (Nicotinamide Riboside Chloride, ChromaDex, #00014332), 1 mM NMN (β-Nicotinamide

525 mononucleotide, Sigma, #N3501, 100 μ M FK-866 (Sigma, #F8557), 1 mM NAM (NAM^{high}),
526 100 μ M NAM (NAM^{Low}), 1 μ M ICG-001 (R&D Systems, #4505/10), 1 μ M IQ-1 (Sigma,
527 #412400), 25 μ M LY364947 (Sigma #L6293), 1 μ M wortmannin (Sigma, #W1628), 100 μ M
528 LY294002 (Sigma, #L9908), 1 μ M SC79 (Sigma, # SML0749), 8 μ M TAK-715 (Sigma,
529 #SML0360), 200 ng/ml WNT3A (R&D Systems, 5036-WN-010/CF) or 1 μ M MK-2206
530 (Selleckchem, #S1078). Immunocytochemistry and image acquisition were performed as
531 described in the Supplementary Information.

532

533 **Other cellular assays**

534 Cellular assays with primary mouse cells and human primary fibroblasts are described in the
535 Supplementary Information.

536

537 **In vivo mouse experiments**

538 Mice were housed under standard conditions (up to 5 mice per cage) and allowed access to
539 food and water *ad libitum*. Young (12-13 weeks-old) and aged (23-25 months-old) wild type
540 C57BL/6JRj males were purchased from Janvier labs. All mice were randomized to different
541 groups according to their weights. Treatments resuspended in 1% Sodium Carboxymethyl
542 cellulose (CMC) were administrated by daily oral gavage, starting prior to the injury and
543 continuing until the endpoint of the study: NAM (200mg/kg per day, Enamine, #EN300-
544 15612), PN (4mg/kg day, Enamine, #EN300-39851), or nicotinamide riboside (NR, 200mg/kg
545 per day, ChromaDex, #00014332). Vehicle-treated mice received an equivalent volume of 1%
546 CMC using the same dosing scheme every day (bolus of 200 μ l maximum performed at the
547 same time of the morning \pm 2 hours). For regeneration studies, muscle injury was induced by
548 intramuscular injection of 20 μ M cardiotoxin (CTX, Latoxan) into the *Tibialis anterior* (TA,
549 25 μ l) and the *Gastrocnemius* (GC, 50 μ l) muscles under anesthesia. For longitudinal muscle

550 strength measurement, muscle injury was induced through eccentric contractions induced by
551 electrical stimulations following a previously published protocol (34) that was adapted as
552 described in the Supplementary Information. Tissue harvesting and immunohistochemistry
553 were performed as detailed in Supplementary Methods. Muscle sections were imaged using the
554 VS120 and VS200 slide scanners (Olympus). Images were analyzed using the VS-ASW FL
555 measurement tool and the QuPath software. For ex vivo assays, MuSCs were isolated with a
556 Beckman Coulter Astrios Cell sorter as previously described (20). MuSC fate was assessed
557 with PAX7 and MYOD immunostainings. Images were acquired using the ImageXpress
558 (Molecular Devices) platform and quantifications were performed using Multi-Wavelength
559 Cell scoring.

560

561 **Human nutritional epidemiology study (Bushehr Elderly Health)**

562 186 older men aged above 60 years and above were randomly selected from the Bushehr
563 Elderly Health (BEH) cohort for a metabolomic sub-analysis (a detailed description of the
564 entire cohort is available elsewhere (47, 71)). The appendicular lean mass index (ALMi) was
565 used as an estimate of skeletal muscle mass using dual energy X-ray absorptiometry and
566 calculated for each participant as the sum of upper and lower limb lean mass expressed in
567 kilogram divided the height square expressed in meter. Physical performance was evaluated
568 using a 4.57-m gait speed test, with gait speed determined as the best of two repeats at the
569 subject's normal pace. An overnight fasting venous blood sample was collected by trained
570 nurses for every participant and serum was stored at -80°C before being analyzed as described
571 under the section "metabolomics analyses".

572

573 **Molecular and biochemical assays**

574 Experiments were performed according to manufacturer's protocols. All experimental
575 procedures and reagents are described in the Supplemental Information file.

576

577 **Statistics**

578 Unless otherwise stated, data were analyzed using the Prism 9 software package and
579 represented as mean \pm SEM. All analyses were performed using parametric statistics based on
580 historical values of the lab. Across all figures, statistical significance is represented using
581 asterisks: * $P \leq 0.05$; ** $P \leq 0.01$; *** $P \leq 0.001$; **** $P \leq 0.0001$. Nonsignificant differences are
582 labeled as "n.s". A Student t-test was used to compare experimental conditions with only two
583 groups and 1-way ANOVA was used to compare experimental conditions with multiple groups
584 using a Dunnett post-hoc test to compare every group to a control and a Tukey post-hoc or
585 Holm-Šidák post hoc test to compare several groups. The Kolmogorov-Smirnov (KS) test was
586 used to compare the cumulative distribution. Brown-Forsythe and Welch's ANOVA test was
587 used when groups do not have equal variances. For human serum analyses, concentrations of
588 NAM and PLP were log₂ and z-score (mean centering and dividing by the standard deviation)
589 transformed, while age was z-score transformed. Multiple linear regressions adjusted for age
590 were performed using R software to estimate the association between clinical response
591 variables (ALM and gait speed) and z-scores of NAM, PLP, dietary intake and age. Statistical
592 analyses of RNA-sequencing experiments is described in the Supplementary Information file.

593

594 **Study approval**

595 Approbation to use human cells for research purposes was obtained from the Vaud ethics
596 commission for human research (CER-VD) under authorization PB_2016-00709. Animal
597 experiments were authorized by the Veterinary office of the Canton of Vaud, Switzerland

598 (authorization no. 3440 and 3690) and both the local ethic committee CEEA-55 and the French
599 ministry of research (APAFIS#30000-2021022210224394 v1). Humane termination endpoints
600 have been established prior to the start of the experiments as described in the animal
601 authorizations. The Bushehr Elderly Health (BEH) cohort consists of 3000 individuals aged
602 over 60 years old and living around the city of Bushehr, Iran. A detailed description of the
603 entire cohort is available elsewhere (47, 71). The study protocol was approved by the ethics
604 committee of Endocrinology and Metabolism Research Institute, affiliated to Tehran
605 University of Medical Science as well as the Research Ethics Committee of Bushehr University
606 of Medical Sciences under reference TUMS.EMRI.REC.1394.0036. Re-analysis performed in
607 Switzerland were approved by the cantonal ethics commission for human research (CER-VD)
608 in Vaud, Switzerland under reference 490/14. A written informed consent was signed by all
609 the participants.

610

611 **Data and materials availability**

612 All software used were freely or commercially available. Any additional information required
613 to reanalyze the data reported in this paper is available upon justified request. RNA sequencing
614 data have been deposited to GEO under accession numbers GSE264284, GSE264285 and
615 GSE269250. Other materials are available for sharing upon justified request within the limit of
616 availability of non-renewable samples. A Supporting Data Values file with all reported data
617 values is available as part of the supplemental material. Complete unedited gel images are
618 provided in the Supplemental Information file.

619

620 **Author contributions**

621 S.A., J.M., P.S, and J.N.F. designed the experimental strategy, interpreted the results, and wrote
622 the manuscript. S.A., J.M., S.K., P.G., S.R., T.D., L.P., J.L.S.G., and P.S. performed

623 experiments and analyzed data. J.M., S.K., Y.R., B.B., and D.B. developed and/or performed
624 the cellular screen. C.J., A.F., R.M., and J.G. designed, performed and analyzed the in vivo
625 muscle contraction experiments. I.S. performed and analyzed β -catenin luciferase experiments.
626 E.M., A.O., R.H. F.F. and J.N.F. lead human metabolomics and analyzed/interpreted the
627 results. S.M. and E.M. performed and analyzed transcriptomic experiments. G.J., L.T., and
628 S.M. supported imaging, flow cytometry, and genomics. L.G.K. and S.B. contributed to
629 experimental strategy and data interpretation. P.S, and J.N.F. conceived and lead the project.
630 S.A. and J.M. are listed as co-first authors as both authors share primary responsibility in
631 conducting experiments, analyses, and interpretation of results for this study. The order of
632 shared authorship reflects the contribution to writing and editing of the manuscript. All authors
633 read and approved the final manuscript.

634

635 **Acknowledgements**

636 We thank Florian Bentzinger for his contribution in the early ideation of the project, and are
637 grateful to Claudia Roessle, Carles Cantó, Omid Mashinchian and the NIHS community for
638 critical discussions of the results and their translational applications. We also thank the
639 Histology Core Facility (HCF) and the Center of Phenogenomics (CPG) at the Ecole
640 Polytechnique Federale de Lausanne (EPFL) for technical support, and MS-Omics (Denmark)
641 and BEVITAL (Norway) for metabolomics analyses. This work was funded by Nestle
642 Research and Nestle Health Science.

643

644 **Competing interests**

645 All authors, except C.J., A.F., R.M., J.G, I.S., A.O., R.H. and F.F., are or were employees of
646 Nestlé (Société des Produits Nestlé SA or Nestlé Health Science SA). Other authors declare
647 no conflict of interest.

648 **REFERENCES**

649

- 650 1. Dumont NA, et al. Satellite Cells and Skeletal Muscle Regeneration. *Compr Physiol.*
651 2015;5(3):1027–59.
- 652 2. Mackey AL, et al. Assessment of satellite cell number and activity status in human skeletal muscle
653 biopsies. *Muscle Nerve.* 2009;40(3):455–65.
- 654 3. Ance S, Stuelsatz P, Feige JN. Muscle Stem Cell Quiescence: Controlling Stemness by Staying
655 Asleep. *Trends Cell Biol.* 2021;31(7):556–568.
- 656 4. Keefe AC, et al. Muscle stem cells contribute to myofibres in sedentary adult mice. *Nat Commun.*
657 2015;6(1):7087.
- 658 5. Snijders T, et al. Satellite cells in human skeletal muscle plasticity. *Front Physiol.* 2015;6:283.
- 659 6. Blaauw B, Reggiani C. The role of satellite cells in muscle hypertrophy. *J Muscle Res Cell Motil.*
660 2014;35(1):3–10.
- 661 7. García-Prat L, Sousa-Victor P, Muñoz-Cánoves P. Proteostatic and Metabolic Control of Stemness.
662 *Cell Stem Cell.* 2017;20(5):593–608.
- 663 8. Soro-Arnáiz I, et al. GLUD1 determines murine muscle stem cell fate by controlling mitochondrial
664 glutamate levels. *Developmental Cell.* 2024;0(0). <https://doi.org/10.1016/j.devcel.2024.07.015>.
- 665 9. Beaudry KM, et al. Nutritional Regulation of Muscle Stem Cells in Exercise and Disease: The Role
666 of Protein and Amino Acid Dietary Supplementation. *Front Physiol.* 2022;13.
667 <https://doi.org/10.3389/fphys.2022.915390>.
- 668 10. Cerletti M, et al. Short-term calorie restriction enhances skeletal muscle stem cell function. *Cell*
669 *Stem Cell.* 2012;10(5):515–519.
- 670 11. Ryall JG, Schertzer JD, Lynch GS. Cellular and molecular mechanisms underlying age-related
671 skeletal muscle wasting and weakness. *Biogerontology.* 2008;9(4):213–28.
- 672 12. Cruz-Jentoft AJ, Sayer AA. Sarcopenia. *Lancet.* 2019;393(10191):2636–2646.
- 673 13. Kedlian VR, et al. Human skeletal muscle aging atlas. *Nat Aging.* 2024;4(5):727–744.
- 674 14. Sousa-Victor P, García-Prat L, Muñoz-Cánoves P. Control of satellite cell function in muscle
675 regeneration and its disruption in ageing. *Nat Rev Mol Cell Biol.* 2022;23(3):204–226.
- 676 15. Blau HM, Cosgrove BD, Ho AT. The central role of muscle stem cells in regenerative failure with
677 aging. *Nat Med.* 2015;21(8):854–62.
- 678 16. Mashinchian O, et al. The Muscle Stem Cell Niche in Health and Disease. *Curr Top Dev Biol.*
679 2018;126:23–65.
- 680 17. Chakkalakal JV, et al. The aged niche disrupts muscle stem cell quiescence. *Nature.*
681 2012;490(7420):355–60.
- 682 18. Moiseeva V, et al. Senescence atlas reveals an aged-like inflamed niche that blunts muscle
683 regeneration. *Nature.* 2023;613(7942):169–178.
- 684 19. Vinel C, et al. The exerkin apelin reverses age-associated sarcopenia. *Nat Med.* 2018;24(9):1360–
685 1371.
- 686 20. Lukjanenko L, et al. Aging Disrupts Muscle Stem Cell Function by Impairing Matricellular WISP1
687 Secretion from Fibro-Adipogenic Progenitors. *Cell Stem Cell.* 2019;24(3):433–446.e7.
- 688 21. Lukjanenko L, et al. Loss of fibronectin from the aged stem cell niche affects the regenerative
689 capacity of skeletal muscle in mice. *Nat Med.* 2016;22(8):897–905.
- 690 22. García-Prat L, et al. Autophagy maintains stemness by preventing senescence. *Nature.*
691 2016;529(7584):37–42.

- 692 23. Palla AR, et al. Inhibition of prostaglandin-degrading enzyme 15-PGDH rejuvenates aged muscle
693 mass and strength. *Science*. 2021;371(6528). <https://doi.org/10.1126/science.abc8059>.
- 694 24. Zhang H, et al. NAD⁺ repletion improves mitochondrial and stem cell function and enhances life
695 span in mice. *Science*. 2016;352(6292):1436–43.
- 696 25. Cosgrove BD, et al. Rejuvenation of the muscle stem cell population restores strength to injured
697 aged muscles. *Nat Med*. 2014;20(3):255–64.
- 698 26. Bernet JD, et al. p38 MAPK signaling underlies a cell-autonomous loss of stem cell self-renewal in
699 skeletal muscle of aged mice. *Nat Med*. 2014;20(3):265–71.
- 700 27. Price FD, et al. Inhibition of JAK-STAT signaling stimulates adult satellite cell function. *Nat Med*.
701 2014;20(10):1174–81.
- 702 28. Lepper C, Partridge TA, Fan CM. An absolute requirement for Pax7-positive satellite cells in acute
703 injury-induced skeletal muscle regeneration. *Development*. 2011;138(17):3639–46.
- 704 29. Fry CS, et al. Inducible depletion of satellite cells in adult, sedentary mice impairs muscle
705 regenerative capacity without affecting sarcopenia. *Nat Med*. 2015;21(1):76–80.
- 706 30. Kouw IWK, et al. One Week of Hospitalization Following Elective Hip Surgery Induces Substantial
707 Muscle Atrophy in Older Patients. *J Am Med Dir Assoc*. 2019;20(1):35–42.
- 708 31. Kortebein P, et al. Effect of 10 days of bed rest on skeletal muscle in healthy older adults. *JAMA*.
709 2007;297(16):1772–1774.
- 710 32. Saba JA, et al. Translational control of stem cell function. *Nat Rev Mol Cell Biol*. [published online
711 ahead of print: July 16, 2021]. <https://doi.org/10.1038/s41580-021-00386-2>.
- 712 33. Laumonier T, et al. Human myogenic reserve cells are quiescent stem cells that contribute to muscle
713 regeneration after intramuscular transplantation in immunodeficient mice. *Sci Rep*. 2017;7(1):3462.
- 714 34. Bernard C, et al. Kinetics of skeletal muscle regeneration after mild and severe muscle damage
715 induced by electrically-evoked lengthening contractions. *The FASEB Journal*. 2023;37(9):e23107.
- 716 35. Goody MF, Henry CA. A need for NAD⁺ in muscle development, homeostasis, and aging. *Skelet*
717 *Muscle*. 2018;8(1):9.
- 718 36. Kulikova V, et al. Degradation of Extracellular NAD(+) Intermediates in Cultures of Human
719 HEK293 Cells. *Metabolites*. 2019;9(12). <https://doi.org/10.3390/metabo9120293>.
- 720 37. Kropotov A, et al. Equilibrative Nucleoside Transporters Mediate the Import of Nicotinamide
721 Riboside and Nicotinic Acid Riboside into Human Cells. *Int J Mol Sci*. 2021;22(3):1391.
- 722 38. Meng Y, et al. Nicotinamide Promotes Cell Survival and Differentiation as Kinase Inhibitor in
723 Human Pluripotent Stem Cells. *Stem Cell Reports*. 2018;11(6):1347–1356.
- 724 39. Liu C, et al. Control of beta-catenin phosphorylation/degradation by a dual-kinase mechanism. *Cell*.
725 2002;108(6):837–47.
- 726 40. Mouradian S, et al. LSD1 controls a nuclear checkpoint in Wnt/ β -Catenin signaling to regulate
727 muscle stem cell self-renewal. *Nucleic Acids Res*. 2024;gkae060.
- 728 41. Teo JL, Kahn M. The Wnt signaling pathway in cellular proliferation and differentiation: A tale of
729 two coactivators. *Adv Drug Deliv Rev*. 2010;62(12):1149–55.
- 730 42. Emami KH, et al. A small molecule inhibitor of beta-catenin/CREB-binding protein transcription
731 [corrected]. *Proc Natl Acad Sci U S A*. 2004;101(34):12682–7.
- 732 43. Miyabayashi T, et al. Wnt/beta-catenin/CBP signaling maintains long-term murine embryonic stem
733 cell pluripotency. *Proc Natl Acad Sci U S A*. 2007;104(13):5668–73.
- 734 44. Schiaffino S, Mammucari C. Regulation of skeletal muscle growth by the IGF1-Akt/PKB pathway:
735 insights from genetic models. *Skelet Muscle*. 2011;1(1):4.

- 736 45. Wolf D, et al. Acetylation of β -Catenin by CREB-binding Protein (CBP) *. *Journal of Biological*
737 *Chemistry*. 2002;277(28):25562–25567.
- 738 46. Grima-Terrén M, et al. Muscle aging and sarcopenia: The pathology, etiology, and most promising
739 therapeutic targets. *Mol Aspects Med*. 2024;100:101319.
- 740 47. Shafiee G, et al. Bushehr Elderly Health (BEH) programme: study protocol and design of
741 musculoskeletal system and cognitive function (stage II). *BMJ Open*. 2017;7(8):e013606.
- 742 48. Studenski S, et al. Gait speed and survival in older adults. *Jama*. 2011;305(1):50–8.
- 743 49. Calderon-Ospina CA, Nava-Mesa MO, Paez-Hurtado AM. Update on Safety Profiles of Vitamins
744 B1, B6, and B12: A Narrative Review. *Ther Clin Risk Manag*. 2020;16:1275–1288.
- 745 50. Knip M, et al. Safety of high-dose nicotinamide: a review. *Diabetologia*. 2000;43(11):1337–45.
- 746 51. Mackey AL, et al. Activation of satellite cells and the regeneration of human skeletal muscle are
747 expedited by ingestion of nonsteroidal anti-inflammatory medication. *FASEB J*. 2016;30(6):2266–
748 2281.
- 749 52. He WA, et al. NF- κ B-mediated Pax7 dysregulation in the muscle microenvironment promotes
750 cancer cachexia. *J Clin Invest*. 2013;123(11):4821–35.
- 751 53. Espino-Gonzalez E, et al. Impaired skeletal muscle regeneration in diabetes: From cellular and
752 molecular mechanisms to novel treatments. *Cell Metab*. 2024;S1550-4131(24)00060–3.
- 753 54. Dumont NA, Rudnicki MA. Targeting muscle stem cell intrinsic defects to treat Duchenne muscular
754 dystrophy. *NPJ Regen Med*. 2016;1:16006-.
- 755 55. da Silva VR, Gregory JF. Chapter 13 - Vitamin B6. In: Marriott BP, et al., eds. *Present Knowledge*
756 *in Nutrition (Eleventh Edition)*. Academic Press; 2020:225–237.
- 757 56. Li H, et al. Lactoferrin Induces the Synthesis of Vitamin B6 and Protects HUVEC Functions by
758 Activating PDXP and the PI3K/AKT/ERK1/2 Pathway. *Int J Mol Sci*. 2019;20(3).
759 <https://doi.org/10.3390/ijms20030587>.
- 760 57. Liu GY, et al. Effects of dietary vitamin B6 on the skeletal muscle protein metabolism of growing
761 rabbits. *Animal Production Science*. 2017;57(10):2007–2015.
- 762 58. Mascolo E, et al. Vitamin B6 rescues insulin resistance and glucose-induced DNA damage caused
763 by reduced activity of Drosophila PI3K. *J Cell Physiol*. 2022;237(9):3578–3586.
- 764 59. Cantó C, Menzies KJ, Auwerx J. NAD(+) Metabolism and the Control of Energy Homeostasis: A
765 Balancing Act between Mitochondria and the Nucleus. *Cell Metab*. 2015;22(1):31–53.
- 766 60. Liu L, et al. Quantitative analysis of NAD synthesis-breakdown fluxes. *Cell Metab*.
767 2018;27(5):1067-1080.e5.
- 768 61. Teo JL, et al. Specific inhibition of CBP/beta-catenin interaction rescues defects in neuronal
769 differentiation caused by a presenilin-1 mutation. *Proc Natl Acad Sci U S A*. 2005;102(34):12171–6.
- 770 62. Brack AS, et al. A temporal switch from notch to Wnt signaling in muscle stem cells is necessary
771 for normal adult myogenesis. *Cell Stem Cell*. 2008;2(1):50–9.
- 772 63. Otto A, et al. Canonical Wnt signalling induces satellite-cell proliferation during adult skeletal
773 muscle regeneration. *J Cell Sci*. 2008;121(Pt 17):2939–50.
- 774 64. Murphy MM, et al. Transiently active Wnt/ β -catenin signaling is not required but must be silenced
775 for stem cell function during muscle regeneration. *Stem Cell Reports*. 2014;3(3):475–88.
- 776 65. Parisi A, et al. APC is required for muscle stem cell proliferation and skeletal muscle tissue repair.
777 *J Cell Biol*. 2015;210(5):717–26.
- 778 66. Rudolf A, et al. β -Catenin Activation in Muscle Progenitor Cells Regulates Tissue Repair. *Cell Rep*.
779 2016;15(6):1277–90.

- 780 67. Roman W, et al. Muscle repair after physiological damage relies on nuclear migration for cellular
781 reconstruction. *Science*. 2021;374(6565):355-359.
- 782 68. Konz T, et al. Sex-Specific Associations of Blood-Based Nutrient Profiling With Body Composition
783 in the Elderly. *Front Physiol*. 2018;9:1935.
- 784 69. Zhang JH, Chung TD, Oldenburg KR. A Simple Statistical Parameter for Use in Evaluation and
785 Validation of High Throughput Screening Assays. *J Biomol Screen*. 1999;4(2):67–73.
- 786 70. Le Moal E, et al. Apelin stimulation of the vascular skeletal muscle stem cell niche enhances
787 endogenous repair in dystrophic mice. *Sci Transl Med*. 2024;16(739):eabn8529.
- 788 71. Ostovar A, et al. Bushehr Elderly Health (BEH) Programme, phase I (cardiovascular system). *BMJ*
789 *Open*. 2015;5(12):e009597.
- 790

791 **TABLES**

792

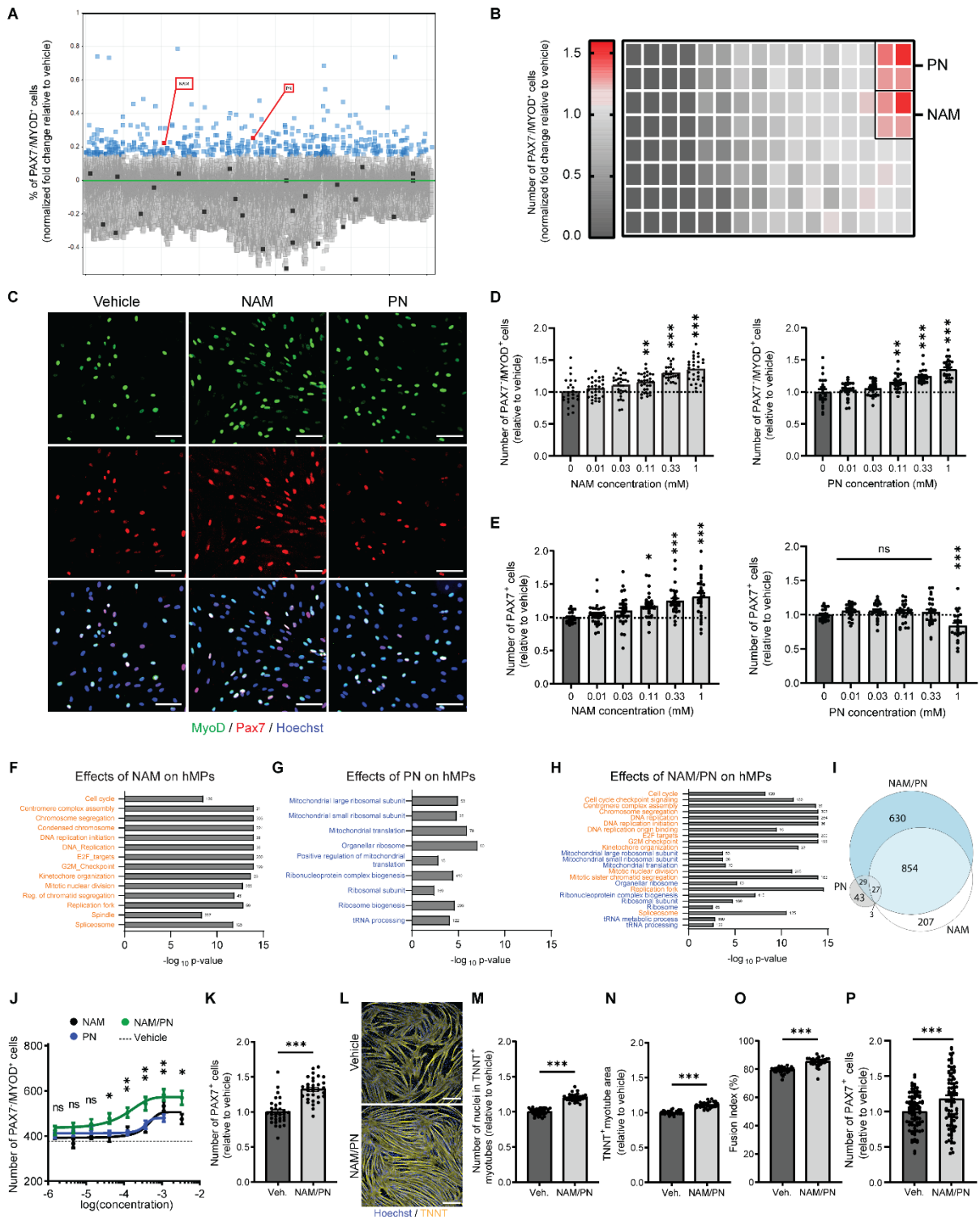
793 **Table 1: Demographic data of the subset of the Bushehr Elderly Health (BEH) cohort (n=186).**
 794 Abbreviations: NAM, nicotinamide; PLP, pyridoxal-5'-phosphate; ALM, appendicular lean mass; BMI,
 795 body mass index.

796

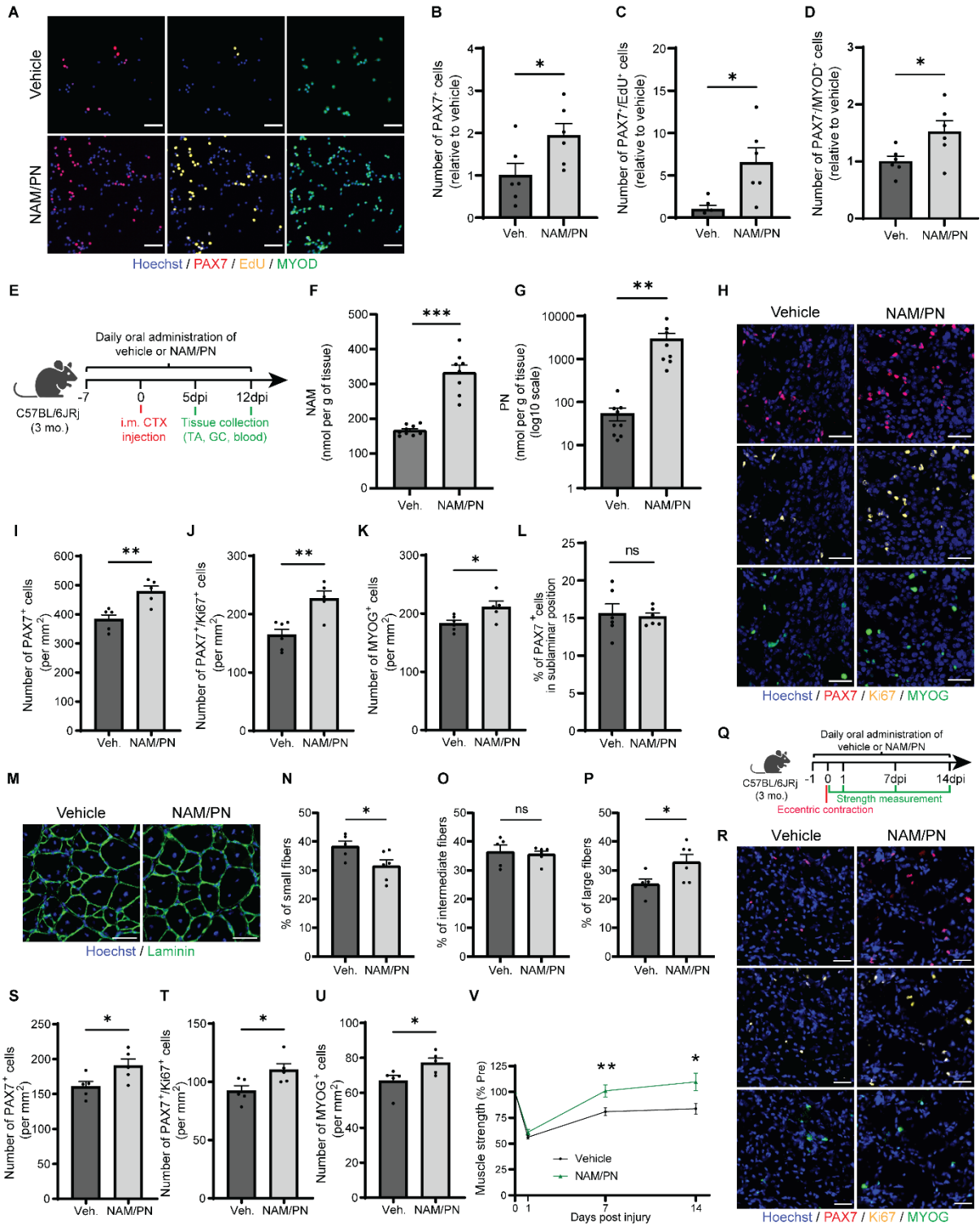
Variable	Mean	SD
Age (years)	68.97	6.17
NAM (nM)	7.49	0.69
PLP (nM)	5.31	0.7
ALM index (kg/m ²)	6.84	0.86
Gait speed (m/s)	0.97	0.3
Weight (kg)	73.49	11.46
Height (m)	1.66	0.06
BMI	26.67	3.58

Variable	Count	%
Sarcopenic (EWGSOP)	84	46.2

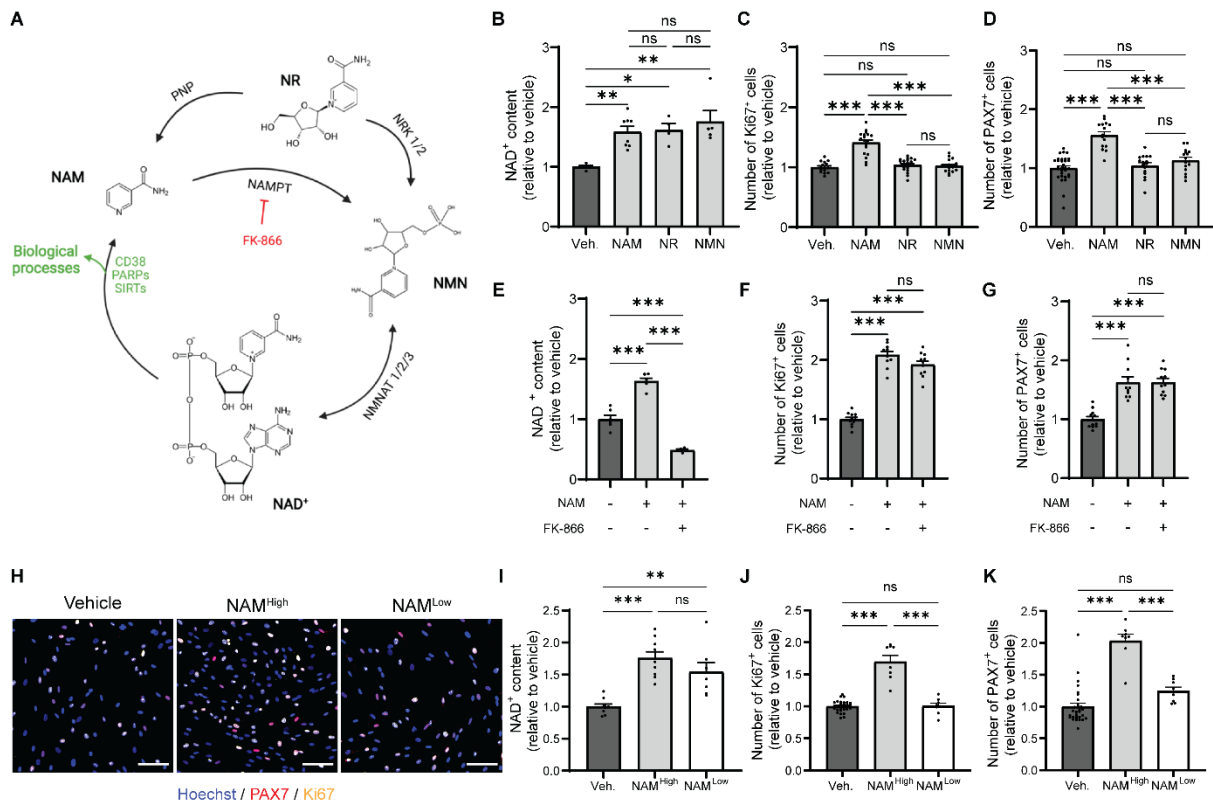
797



801 **Fig. 1. A high-content screen identifies NAM and PN as activators of hMP amplification**
802 **and differentiation.** (A) Percentage of PAX7⁻/MYOD⁺ hMPs after 72h treatment with 50,000
803 bioactive molecules. Min-Max normalization between negative (black line) and positive
804 control (LY363947, green line) was performed. Blue: compounds with normalized effect size
805 > 15%; black: Generally Recognized As Safe (GRAS) molecules; red: GRAS hits. (B) Relative
806 number of PAX7⁻/MYOD⁺ cells in hMPs treated with GRAS-classified molecules. n = 2-4 cell
807 culture replicates from N = 2 donors. (C) Representative images of hMPs treated with vehicle,
808 NAM, or PN for 72h. Scale bar, 100 μm. (D, E) Dose-response of NAM and PN on the relative
809 number of PAX7⁻/MYOD⁺ (D) and PAX7⁺ (E) hMPs treated with vehicle, NAM, or PN for
810 72h. n ≥ 21 cell culture replicates from N = 2 donors. (F-H) Gene set enrichment analysis of
811 upregulated gene sets in hMPs treated with NAM (F), PN (G), or NAM/PN combination (H)
812 compared to vehicle. False discovery rate: 10%. N = 5 donors. (I) Venn diagram of upregulated
813 genes using 5% FDR multiple testing correction. (J) Dose-response of NAM, PN, and
814 NAM/PN on PAX7⁻/MYOD⁺ hMPs. n ≥ 6 cell culture replicates from one donor. (K)
815 Quantification of PAX7⁺ hMPs after vehicle and NAM/PN treatment. n ≥ 32 cell culture
816 replicates from one donor. (L-O) Representative images (L) and quantification of nuclei within
817 myotubes (M), myotube area (N), and fusion index (O) in hMPs treated with vehicle or
818 NAM/PN during proliferation and differentiation. Scale bar, 500 μm. n ≥ 28 cell culture
819 replicates for each condition from one donor. (P) Quantification of PAX7⁺ hMPs after vehicle
820 and NAM/PN treatment post myotube differentiation induction. n ≥ 92 cell culture replicates
821 from one donor. Data represent means ± s.e.m. *** P<0.001; ** P<0.01, * P<0.05 with one-
822 way ANOVA followed by post hoc Dunnett's (D,E) or Tukey's (J) multiple comparison test,
823 and two-tailed unpaired Student's t-tests (K,M,N,O,P).
824
825



829 **Fig. 2. The combination of NAM and PN enhances MuSC function in vivo and increases**
830 **muscle strength during regeneration.** (A-D) Representative immunofluorescence images
831 and quantification of FACS-isolated mouse MuSCs treated with vehicle or NAM/PN *ex vivo*
832 for 4 days. n = 6 cell culture replicates with cells pooled from N = 4 mice. (E) Cardiotoxin-
833 induced muscle regeneration in young mice treated orally with NAM/PN or vehicle. (F,G)
834 NAM and PN concentrations quantified by LC-MS/MS in uninjured *Gastrocnemius* (GC)
835 muscles from young vehicle (N = 9) and NAM/PN-treated (N = 8) mice. (H-K) Representative
836 immunofluorescence images (H) and quantification of PAX7⁺ (I), PAX7⁺/Ki67⁺ (J), and
837 MYOGENIN⁺ (K) cells in *Tibialis Anterior* (TA) cross-sections from vehicle (N = 6) and
838 NAM/PN-treated (N = 5) mice at 5 dpi. (L) Number of PAX7⁺ sublaminar MuSCs in TA cross-
839 sections from vehicle (N = 6) and NAM/PN-treated (N = 6) mice at 12 dpi. (M-P)
840 Representative immunofluorescence images (M) and quantification of minimum ferret of small
841 ($\leq 33\mu\text{m}$) (N), intermediate ($>33\mu\text{m}$ and $\leq 43\mu\text{m}$) (O), and large ($>43\mu\text{m}$) (P) regenerating
842 myofibers in TA cross-sections from vehicle (N = 5) and NAM/PN-treated (N = 6) mice at 12
843 dpi. (Q) Eccentric contraction (EC)-induced muscle regeneration after electrically-evoked
844 lengthening contractions of *Plantar Flexor* (PF) muscles in young vehicle- and NAM/PN-
845 treated mice. (R-U) Representative immunofluorescence (R) and quantification of PAX7⁺ (S),
846 Ki67⁺ (T) and MYOGENIN⁺ (U) cells in GC muscle from vehicle (N = 5) and NAM/PN-
847 treated (N = 5) mice 7 days after the EC protocol. (V) Quantification of muscle strength (single
848 twitch peak torque) in PF muscles before and 1, 7, and 14 days after EC-induced injury. N =
849 12 mice. Data represented as means \pm s.e.m. *** $P < 0.001$; ** $P < 0.01$; * $P < 0.05$ with two-
850 tailed unpaired Student's t-tests (B,C,D,F,G,I,J,K,L,N,O,P,S,T,U). Scale bars, 50 μm .
851
852
853
854
855



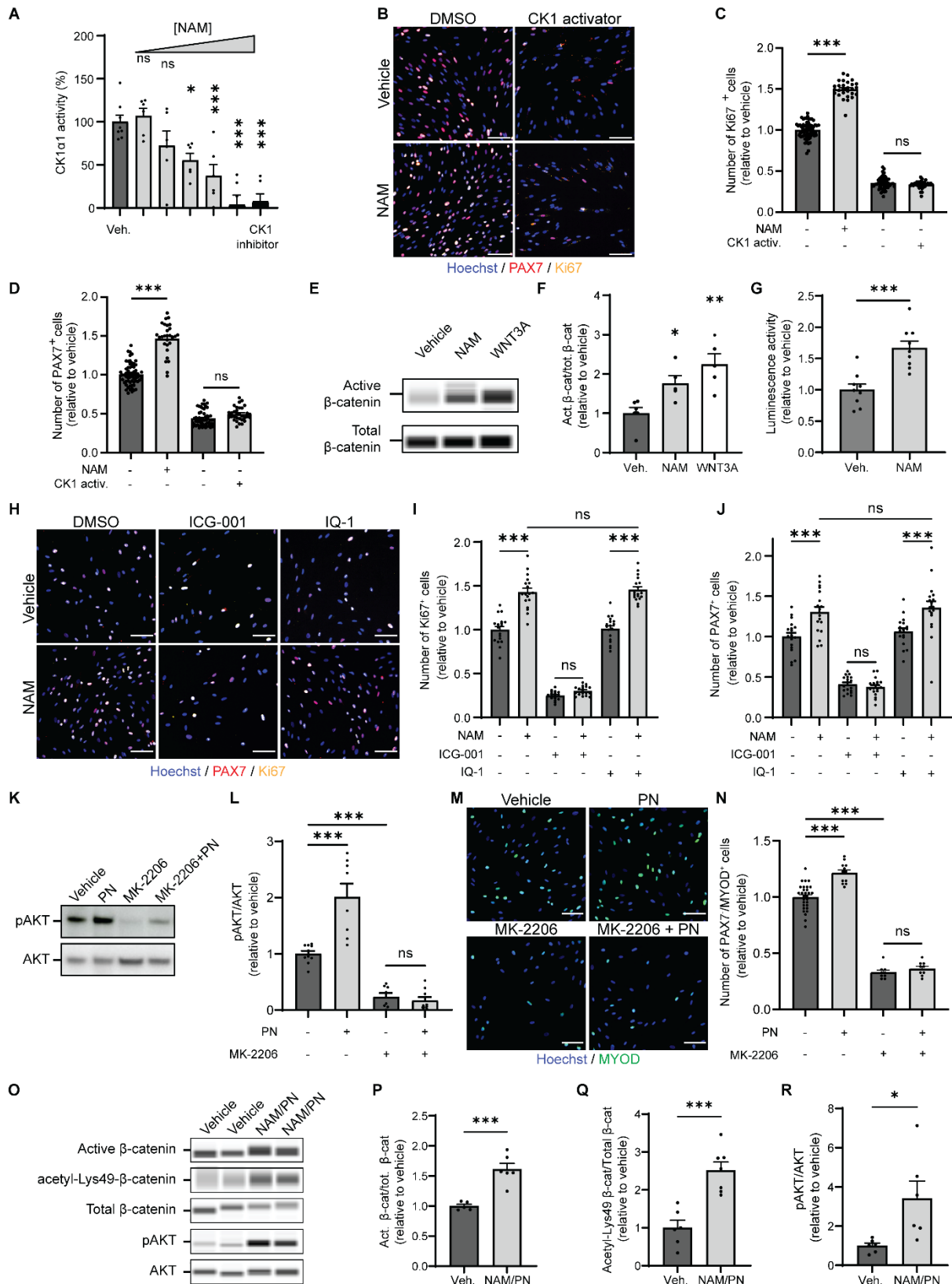
856

857 **Fig. 3. Nicotinamide promotes human myogenic progenitor proliferation independently**
 858 **of NAD⁺ metabolism.** (A) Scheme of mammalian NAD⁺ biosynthesis from various NAD⁺
 859 precursors. NAD⁺, nicotinamide adenine dinucleotide; NR, nicotinamide riboside; NMN,
 860 nicotinamide mononucleotide; NAMPT, nicotinamide phosphoribosyl transferase; NMNAT,
 861 nicotinamide mononucleotide adenylyl transferase; NRK, nicotinamide riboside kinase; PNP,
 862 purine nucleoside phosphorylase. (B-D) NAD⁺ content (B) and number of Ki67⁺ (C) and
 863 PAX7⁺ (D) human myogenic progenitors (hMPs) after treatment with vehicle or different
 864 NAD⁺ precursors. $n \geq 4$, and $n \geq 15$ cell culture replicates per condition from $N = 2$ donors, for
 865 (B) and (C,D), respectively. (E-G) NAD⁺ content (E) and number of Ki67⁺ (F) and PAX7⁺ (G)
 866 hMPs after treatment with NAM and the NAMPT inhibitor FK-866. $n \geq 4$, and $n \geq 11$ cell
 867 culture replicates per condition from $N = 2$ donors, for (E) and (F,G), respectively. (H-K)
 868 Representative pictures (H), NAD⁺ levels (I), and number of Ki67⁺ (J) and PAX7⁺ (K) hMPs
 869 after treatment with NAM at low (100 μM) and high (1 mM) doses. Scale bar, 100 μm. $n \geq 7$
 870 (I), and $n \geq 8$ (J,K) cell culture replicates from one donor. Data represented as means \pm s.e.m.
 871 *** $P < 0.001$; ** $P < 0.01$; * $P < 0.05$. one-way ANOVA with post hoc Tukey's multiple
 872 comparison test (B,C,D,E,F,G,I,J,K).

873

874

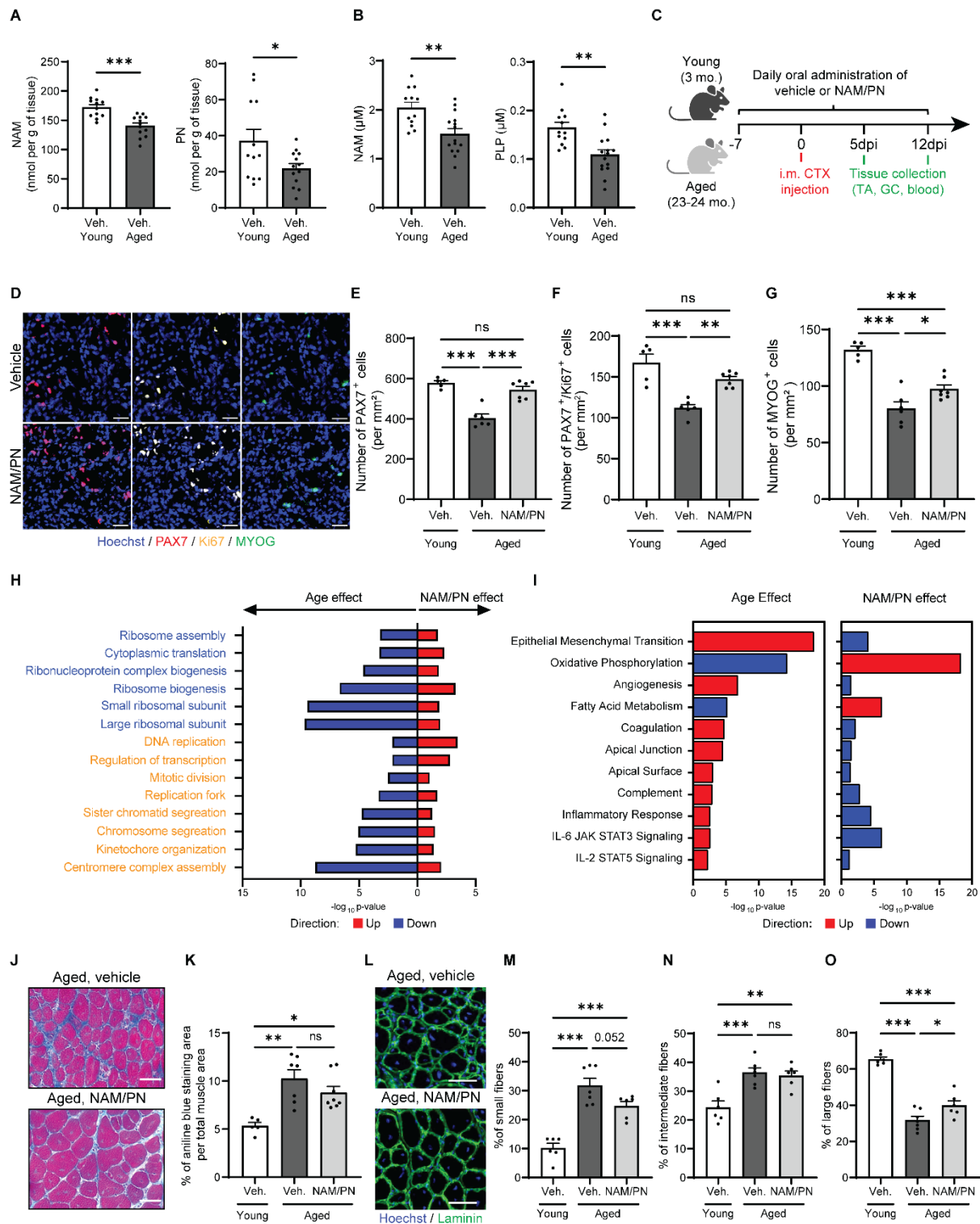
875



876
877

878 **Fig. 4. NAM and PN stimulate hMPs through β -catenin and AKT signaling, respectively.**
879 (A) Dose-response of NAM on CK1 α 1 activity (1 μ M to 20 mM). $n \geq 6$ replicates. (B-D)
880 Representative immunofluorescence images (B) and quantification of Ki67⁺ (C) and PAX7⁺
881 hMPs after treatment with NAM and/or CK1 α activator. $n \geq 16$ cell culture replicates from

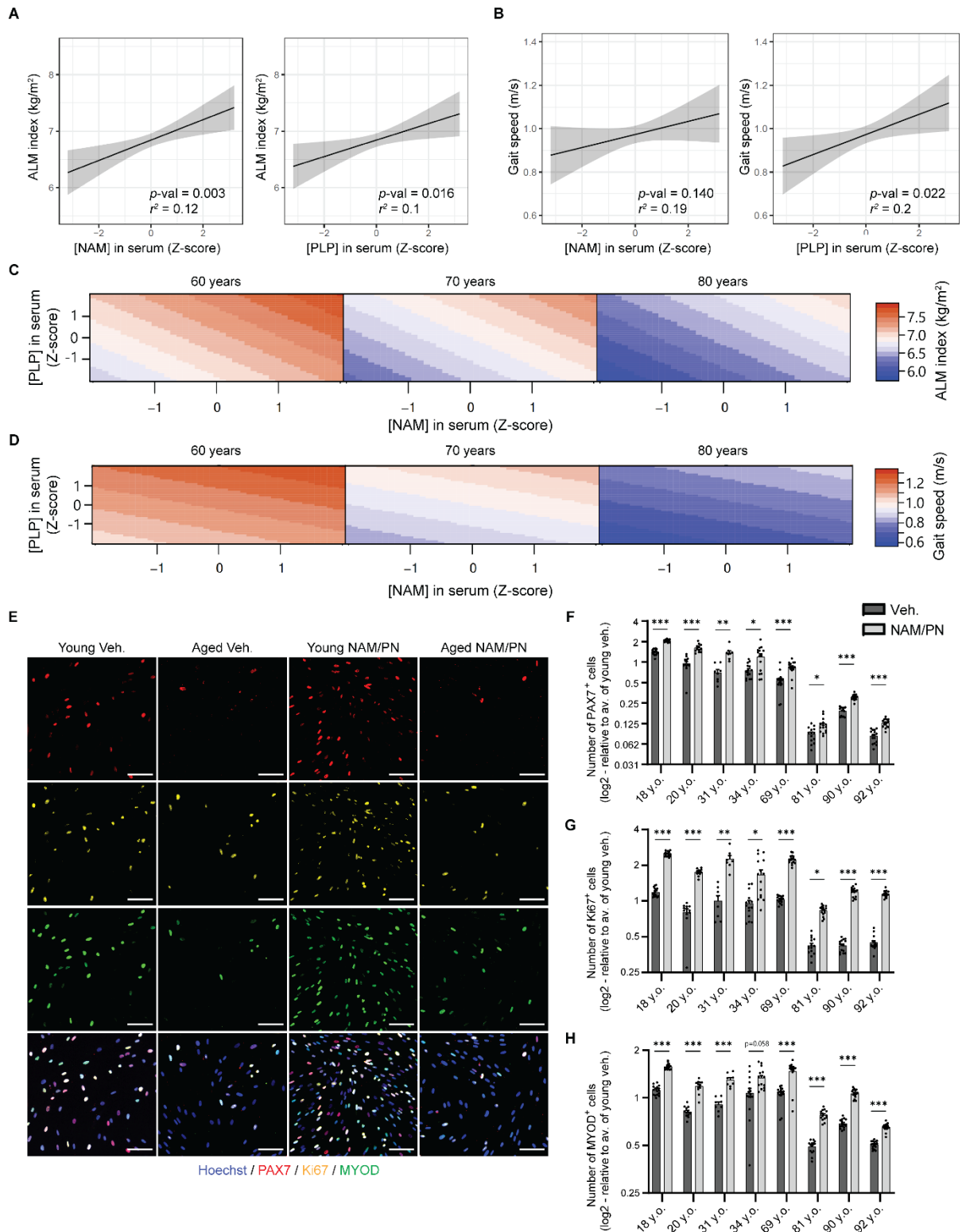
882 one donor. **(E,F)** Representative capillary immunoassays (E) and quantification (F) of non-
883 phosphorylated β -catenin protein levels in NAM-treated hMPs. WNT3A was used as positive
884 control of β -catenin activation. $n \geq 5$ cell culture replicates from $N = 2$ donors. **(G)** Luciferase
885 activity of primary mouse MuSCs co-transfected with a TopFlash β -catenin luciferase reporter
886 gene and treated with vehicle or NAM. $n = 9$ cell culture replicates. **(H-J)** Representative
887 immunofluorescence images (H) and quantification of Ki67⁺ (I) and PAX7⁺ (J) hMPs after
888 treatment with NAM and/or the β -catenin nuclear inhibitors ICG-001 and IQ-1. $n \geq 18$ cell
889 culture replicates from one donor. **(K, L)** Representative immunoblot images (K) and
890 quantification (L) of hMPs treated with PN and/or the AKT inhibitor MK-2206. $n \geq 8$ cell
891 culture replicates from one donor. **(M,N)** Representative immunofluorescence images (M) and
892 quantification of MYOD⁺ hMPs (N) following treatment with PN and/or MK-2206. $n \geq 9$ cell
893 culture replicates from one donor. **(O-R)** Representative capillary immunoassays (O) and
894 quantification of active non-phosphorylated β -catenin protein levels (P), Lys49 acetylation of
895 β -catenin (Q), and pAKT/AKT ratio (R) in MuSCs from regenerating muscles following oral
896 NAM/PN supplementation in young mice. $N \geq 5$ mice for each condition. Mouse MuSCs were
897 freshly isolated from regenerating mouse TA, GC, and QD muscles at 5 dpi. Data represented
898 as means \pm s.e.m. *** $P < 0.001$; ** $P < 0.01$; * $P < 0.05$. One-way ANOVA with post-hoc
899 Dunnett's (A, F), Sidak's multiple comparisons adjustment (C,D,I,J,L,N) or two-tailed
900 unpaired Student's t-test (G,P,Q,R). Scale bars: 100 μ m.
901



902
903
904
905
906
907
908
909
910
911

Fig. 5. NAM/PN restores MuSC function and enhances regeneration in aged skeletal muscle. (A-B) *Gastrocnemius* (A) and plasma (B) concentrations of NAM and PN or NAM and PLP by LC-MS/MS in young and aged mice. $N \geq 12$ mice per group (C) Experimental scheme of CTX-induced muscle regeneration in young and aged mice treated with NAM/PN or vehicle. (D-G) Representative immunofluorescence images (D) and quantification of PAX7⁺, PAX7⁺/Ki67⁺ (F), and MYOGENIN⁺ (G) cells on *Tibialis Anterior* (TA) cross-sections from young ($N = 5$) and aged vehicle- ($N = 6$) and NAM/PN-treated ($N = 7$) mice at 5 dpi. (H) Gene set enrichment analysis (GSEA) curated from GO:BP gene sets of freshly

912 isolated MuSCs from young and aged mice (age effect) and of aged MuSCs treated ex vivo
913 with vehicle or NAM/PN (treatment effect) (N = 6). **(I)** Gene set enrichment analysis of curated
914 Hallmarks gene sets of regenerating GC muscles of young *vs* aged mice and of vehicle- *vs*
915 NAM/PN-treated aged mice 5 dpi (N = 6). False discovery rate: 10%. **(J,K)** Representative
916 images (J) and quantification (K) of fibrotic aniline blue-positive area from a Masson trichrome
917 staining of TA cross-sections from young (N = 5) and aged vehicle- (N = 7) and NAM/PN-
918 treated (N=8) mice at 12 dpi. **(L-O)** Representative immunofluorescence images (L),
919 quantification of minimum ferret myofiber size of small ($\leq 22\mu\text{m}$) (M), intermediate ($>22\mu\text{m}$
920 and $\leq 32\mu\text{m}$) (N), and large ($>32\mu\text{m}$) (O) regenerating myofibers in TA cross-sections from
921 young (N = 6), aged vehicle- (N = 7) and NAM/PN-treated (N = 6) mice at 12 dpi. Data are
922 represented as means \pm s.e.m. *** $P < 0.001$; ** $P < 0.01$; * $P < 0.05$. Two-tailed unpaired
923 Student's t-test (A,B) and one-way ANOVA followed by post hoc Tukey's (E,F,G,K,M,N,O)
924 multiple comparison tests. Scale bars, 50 μm .
925



926
927

928 **Fig. 6. Nicotinamide and pyridoxine associate with muscle mass and function in aged**
929 **humans and restore the myogenic capacity of aged hMPs. (A-D)** LC-MS/MS analyses of
930 NAM and pyridoxal-5'-phosphate (PLP, bioactive pyridoxine) in the serum of men aged > 60
931 years (N = 186 subjects). Appendicular lean mass index (ALMi) (A) and gait speed (B) were
932 correlated to serum concentrations of NAM and PLP using a linear regression model adjusted
933 for age. Regression line (black) and 95% confidence interval (gray). Estimated outcomes of the
934 combined effect of NAM and PLP on ALMi (C) and gait speed (D) were modeled at different
935 ages using a multiple linear regression model adjusted for age. **(E-H)** Representative
936 immunofluorescence images and quantification of PAX7⁺ (F), Ki67⁺ (G) and MYOD⁺ (H)
937 hMPs, n ≥ 8 cell culture replicates from N = 8 donors aged from 18 to 92 years following 72h
938 of treatment with vehicle or NAM/PN. Data presented are means ± s.e.m. *** *P* < 0.001; ** *P*
939 < 0.01. Data are mean ± SEM with significance assessed using Brown-Forsythe and Welch's
940 ANOVA tests with Dunnett T3 multiple-comparison in 8 donors (F,G,H). Scale bar, 100 μm.
941

942